RESPONSE OF CONCRETE PLATES REINFORCED WITH CARBON, BASALT AND STEEL FIBRES UNDER LOADING

CAPOZUCCA Roberto [1], BOSSOLETTI Sonia [2], GABRIELLONI Maria [3]

Abstract

The use of fibres in civil engineering is increasing both in the rehabilitation and in the strengthening of RC elements. An emerging method for retrofitting concrete and masonry walls is the use of thin mortar slabs reinforced with fibre meshes.

This paper analyses the use of concrete embedded carbon, basalt, and steel fibres as substitutes for steel bars to reinforce concrete plates through experimental investigation.

Three, thin, concrete plate specimens measuring 1.0m x 1.0m x 50mm were reinforced with carbon, basalt, and steel fibre meshes, respectively. The fibres were positioned during the casting phase, at a distance of 15mm from the concrete surface. The plates were subjected to the same loading path until failure; the experimental results are discussed and compared with theoretical data. Experimental results showed that the strengthening of concrete plates with fibre meshes is a valid method in practice although bond mechanism influences bending response.

Keywords: concrete plate; carbon, basalt, and steel fibres; bending test

1. Introduction

The use of fibres such as Fibre Reinforced Polymers (FRPs) is increasing in civil engineering especially in the rehabilitation of damaged RC beams or to retrofit RC elements [1-4]. FRPs are available in lamina, strips, tendons, reinforcing bars, and meshes. The techniques usually adopted in the strengthening of RC concrete elements such as beams and columns consist in the use of FRP lamina/strips glued on the concrete surface [1,2] or FRP rods/strips inserted into grooves in the cover of sections [3]. This last technique foresees near surface mounted FRPs and it represents a convenient method for limiting a number of problems linked to the use of externally bonded FRP lamina/strips strengthening. Experimental results confirmed the availability of strengthening with FRPs. Many investigations analysed the possibility of using fibres embedded in cement matrix

[1] CAPOZUCCA Roberto, Associate Professor of Struct. Eng., DICEA, University Politecnica delle Marche, 60100 Ancona, Italy. Ph. +39.071.2204570 Fax +39.071.2204576 e-mail r.capozucca@univpm.it

[2] BOSSOLETTI Sonia, PhD Student, DICEA, University Politecnica Marche, 60100 Ancona, Italy. e-mail s.bossoletti@univpm.it

[3] GABRIELLONI Maria, M. Eng., 60100 Ancona, Italy.

[4,5] to retrofit civil structures; both concrete and masonry. The use of relatively new fibres such as basalt or steel [6-8] employed as substitutes for steel reinforcements is increasing.

This paper describes an experimental investigation carried out to evaluate the bending behaviour of thin, fibre reinforced concrete plates without the use of polymeric matrix; the concrete itself becomes a matrix for the fibres which substitute steel bars in the tensile zone of the plate under loading. Three thin concrete plate specimens measuring 1.0m x 1.0m x 50mm were reinforced with carbon, basal, and steel fibres, respectively, positioned as meshing during the casting of the concrete specimens, on a plane and at a distance of 15mm from the concrete's surface. The plates were subjected to the same loading path until failure. The experimental results are discussed below and compared with theoretical data. The plates' behaviours confirm the availability of using dry fibre mesh in the tensile concrete zone although bond mechanisms have a great influence on response under loading.

2. Experimental texts

2.1 Reinforced Concrete Specimens

Experimental texts were carried out on three thin isotropic concrete plates P1, P2, and P3, measuring 1.0m x 1.0m and thickness t=50mm. The three concrete plates, P1, P2, and P3, were reinforced, respectively, with carbon, basalt, and steel fibres arranged as strip mesh on a plane at a distance of 15mm from the concrete surface.

The fibres were disposed during the casting of the concrete for the construction of the plates (Figures 1(a), 1(b) and 1(c) show the experimental concrete plate specimens with fibres). Plate P1 was reinforced for each edge with 18 20mm wide carbon fibre strips; plate P2 with 18 24mm wide basalt fibre strips; plate P3 with 15 50mm wide steel fibre strips. The area of fibres was ~12mm^2 in each of the specimens for a 200mm interval of length.

Main fibre parameters are shown in Table 1. The concrete used had a compressive strength equal to fc~34.4kN/mm^2 and a tensile strength equal to fct~3N/mm^2.

(a) (b) (c)

Fig. 1: Experimental plates during casting of concrete with fibre mesh: (a) carbon fibre - P1; (b) basalt fibre - P2; (c) steel fibre - P3

2.2 Instruments and loading test

The plates were tested under cycles of vertical centred load, P, distributed on an area with increasing intensity up to failure. The results of the experimental tests are shown in Figure 2. The instruments used during the tests were:

- one loading cell for measuring transmitted load, P, centred on the area of the plate measuring 300mm x 300mm;
- five electronic transducers LVDT for measuring deflections at five points on the bottom surface of the plate (A,…,E) (Figure 3(b));
- four strain gauges located at the centre of the plate, both horizontally and vertically, on the top and bottom concrete surfaces of the plate, in order to measure strains (Figures 3(a) and 3(b)).

Tab.1: Experimental data of carbon, basalt and steel fibres

Fibre	**Strength** f_{fk} (N/mm^2)	**Young's modulus** (N/mm^2)	**Ultimate strain** e_f (%)	**Area** (mm^2/cm)	**Density** ρ
Carbon Fibre	3430	230000	1.50	1.65	1.80g/m^3
Basalt Fibre	3080	95000	3.15	1.40	2.80g/m^3
Steel Fibre	3200	206000	1.60	2.27	1800g/m^2
 Carbon Fibre		 Basalt Fibre		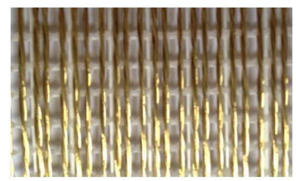 Steel Fibre	

(a) (b)

Fig. 2: (a) Set up of the concrete plates' loading tests; (b) plate surface with deflection measure points (A,…,E) and strains (G,H)

The experimental results obtained by the three tested plates were analysed using the following diagrams: load, P, vs. deflections, δ; load, P, vs. strains, ε; moment, M, vs. curvature, χ. The curvature χ in one plate direction was evaluated from experimental strains using the following relation:

$$c = \frac{e_{c,top}}{x_c} \tag{1}$$

where: $e_{c,top}$ = strain on concrete; x_c = position neutral axis, by the compatibility equation:

$$\frac{e_{c,top}}{x_c} = \frac{e_{c,bottom}}{t - x_c} \quad \text{à} \quad x_c = \frac{e_{c,top}}{e_{c,bottom} + e_{c,top}} \cdot t \tag{2}$$

where $e_{c,top}, e_{c,bottom}$ = strain of top and bottom concrete surfaces; t = height of plate.

2.3 Experimental failure of plates

Concrete plates P1 and P2 showed a similar behaviour with diffused cracking up to failure. In P1 and P2 failure is associated with growing cracking on the bottom surface; failure load values were, respectively, for P1 and P2 plates, equal to 26kN and to 28.70kN (Figures 3(a) and 3(b)).

(a)  (b)

Fig. 3: Cracking failure of (a) concrete plate P1 and (b) P2

Plate P3 showed a diffused cracking state at the bottom concrete surface for load equal to 26kN (Figure 4(a)); subsequently, the plate was able to reach failure load equal to 63.90kN with punching (Figure 4(b)).

(a) 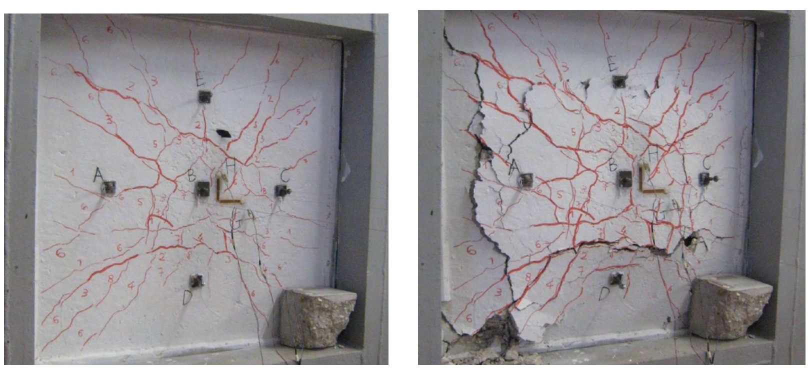 (b)

Fig. 4: (a) Cracking phase of P3 at vertical load P=26kN; (b) punching failure.

3. Theoretical analysis

The non-linear analysis of thin plates was developed to compare theoretical and experimental results. Comparisons are shown below on the base of load, P, vs. displacement, δ, diagrams. Theoretical load, P, vs. displacement, δ, diagrams were evaluated considering two typical steps in the load-displacement behaviour of simply supported thin plates: first, the un-cracked stage up to cracking load; second, the cracking phase up to failure load. The following hypotheses were assumed in the theoretical analysis: planarity of bending section up to failure; perfect bond between reinforcing fibres and concrete; concrete without strength under tensile stress. The behaviour of compressive concrete is characterized by a first elastic branch and a constant curve in the plastic field. Young's modulus was assumed equal to E_c=33945 N/mm^2; limit elastic strain ε_{c0}=0.002

and ultimate strain ε_{cu}=0.0035 [9]. The fibres are characterized by an elastic linear branch. Navier's solution double series was applied [10]; for each increasing load value, the corresponding displacement is evaluated by the following relation:

$$w(x,y)=\frac{16\cdot P}{c\cdot d\cdot p^{6}\cdot D}\cdot\sum_{m=1}^{\infty}\sum_{n=1}^{\infty}\frac{sen\frac{mpu}{a}\cdot sen\frac{npv}{b}\cdot sen\frac{mpc}{2a}\cdot sen\frac{npd}{2b}}{m\cdot n\cdot\left(\frac{m^{2}}{a^{2}}+\frac{n^{2}}{b^{2}}\right)^{2}}\cdot sen\frac{mpx}{a}\cdot sen\frac{npy}{b}\cdot \qquad (1)$$

where: a,b = dimensions of plate; c,d = dimensions of load area; D = bending stiffness of the plate. In plate P1, only one theoretical stiffness was considered. In plates P2 and P3, different stages in the plates' load-displacement behaviour were considered using different values of stiffness. Stiffness values were obtained from experimental diagram of load, P, vs. deflection, δ, recorded during the experimental bending tests. The experimental diagrams of five transducers equipped points were analysed. Different line slopes were determined for each diagram, according to different stages in the load-displacement behaviour of the plates: cracking, failure, and punching. Cracking and failure loads were determined using the inverse relation of the bending moment derived by Navier's method. Cracking moment was evaluated using the following relation (Figure 5(a)):

$$M_{f}=\frac{f_{cfm}\cdot I}{n'\cdot(t-x_{c})} \qquad (2)$$

where: f_{cfm} = average flexural tensile strength of concrete; I = moment of inertia; n' = homogenization ratio; t = thickness of plate. Failure moment was evaluated by the following equilibrium equation (Figure 5(b)):

$$M_{Rd}\cong f_{cd}\cdot 0{,}8x_{c}\cdot b\cdot(d-0{,}4x_{c}) \qquad (3)$$

where: f_{cd} = design strength of concrete; d = distance of fibres to the compressive edge.

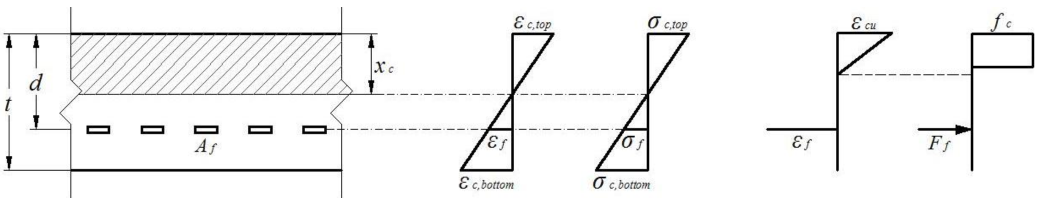

(a) (b)

Fig. 5: Theoretical stress-strain distribution on a section of plate: (a) elastic and (b) inelastic strain-stress distribution.

4. Analysis of results

The main results obtained by the tests described are shown and discussed. Data regarding loading paths and displacements on the three plates allows assessing the validity of reinforcing and the response of plates reinforced with carbon, basalt, and steel fibres. Thin plates were examined under increasing load up to failure.

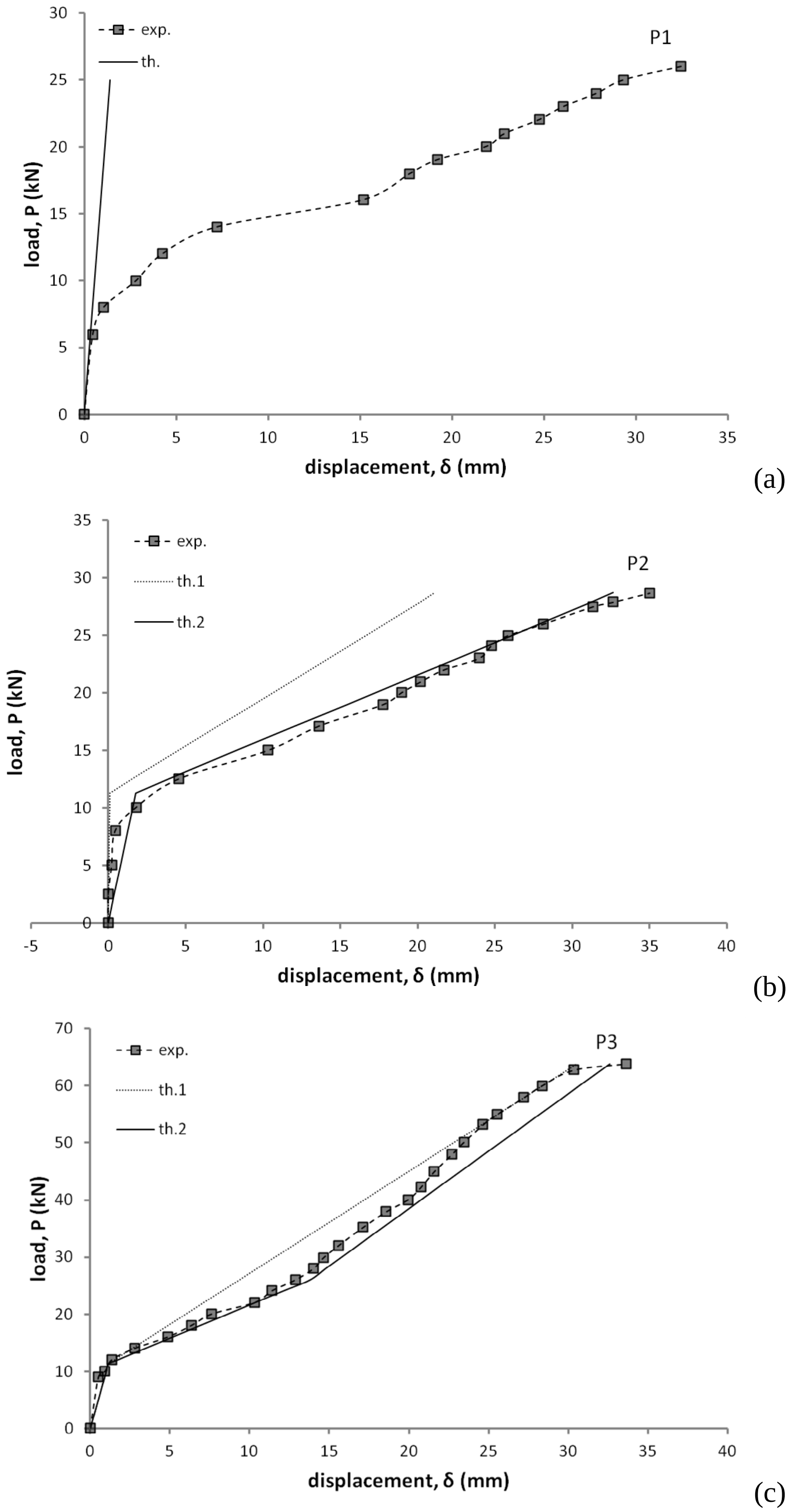

Fig. 6: Comparison between experimental and theoretical load, P, vs. displacement, δ, for (a) P1; (b) P2 and (c) P3 plates.

Figure 6(a) shows a comparison between experimental and theoretical load, P, vs. displacement, δ, for plate P1. The dashed line with squares (referred to as exp. in the legend) describes experimental results; the full line describes theoretical data obtained by Navier's method with initial stiffness of un-cracked concrete. It appears that good agreement with experimental and theoretical data was obtained only in the first linear elastic stage up to cracking.

Figure 6(b) shows a comparison between experimental and theoretical load, P, vs. displacement, δ, for plate P2. The dashed line with squares (referred to as exp. in the legend) describes the experimental results. The solid lines describe the theoretical data obtained by Navier's method: the thin one is obtained considering two medium stiffness values; the thick one is obtained considering two minimum stiffness values. It appears that good agreement with experimental and theoretical data was achieved up to failure, mainly with minimum stiffness values.

Figure 6(c) shows a comparison between experimental and theoretical load, P, vs. displacement, δ, for plate P3. The dashed line with squares describes the experimental results. The full lines describe theoretical data obtained by Navier's method: the thin one is obtained considering two minimum stiffness values; the thick one is obtained considering three minimum stiffness values. It appears to be in good agreement with experimental and theoretical data up to failure, mainly with three minimum stiffness values.

Therefore, in plates P1 and P2, two stages describe the response of reinforced plates: first, linear elastic behaviour up to cracking load; then the cracking of tensile concrete, the second being the inelastic phase, with loss of stiffness, hence, increase of displacement and strain value up to failure load, due to the collapse of compressive concrete. In plate P3 there is a third phase with an increase of stiffness up to punching load, because in this stage only the steel fibres resist.

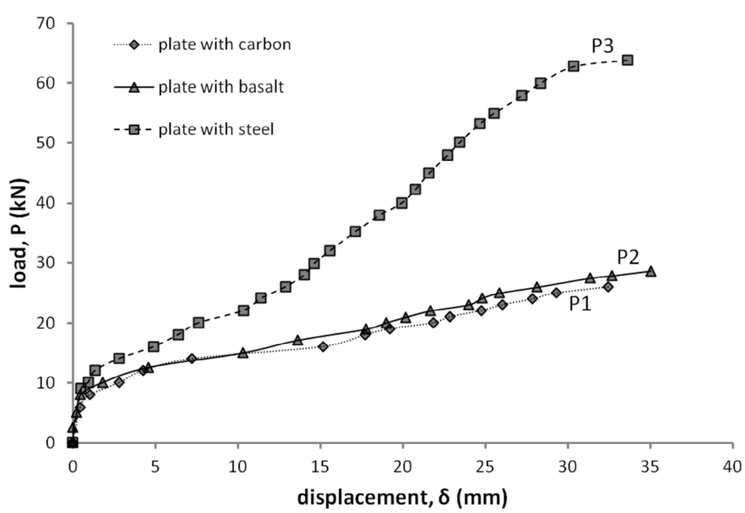

Fig. 7: Comparison of experimental load vs. displacement diagrams at the mid-point of plates P1, P2 and P3.

The experimental results obtained by testing on the plates agree with the theoretical data determined by Navier's semi-linear method.

The different behaviour of the three plates, reinforced with carbon, basalt, and steel fibres, respectively, for P1, P2 and P3, may be analysed in Figure 7, where a comparison of experimental load vs. deflection is shown. Diagrams for reinforced plates P1 and P2 have a similar trend with initial value of cracking load equal to about 11.30kN, and failure load, respectively, equal to 26kN and 28.70kN.

Reinforced plate P3 shows the same initial cracking load and successively an increase of stiffness; at the same failure displacement the ultimate load of plate P3 (63.90kN) is about 2.5 times greater than that of the value recorded for P1 and P2.

5. Conclusions

The bending response of thin concrete plates reinforced with carbon, basalt, and steel fibres was investigated experimentally. The following conclusions can be drawn from the experimental results:

1. The use of composite fibre strips is a valid method for reinforcing thin concrete plates, instead of steel bars;

2. The failure was governed for all plates by the collapse of compressive concrete;

3. Plates P1 and P2, concrete reinforced with carbon and basalt fibres, had a similar bending response with similar displacements, because fibres have the same bond in concrete;

4. Plate P3, concrete reinforced with steel fibres, showed low displacements and a high strength due to an adequate adhesion of the steel fibres with the concrete;

5. The experimental test results are close to the theoretical data obtained by a semi-linear method developed by Navier's solution double series for thin plates.

Acknowledgements

This research was supported by research funds by Università Politecnica delle Marche.

References

[1] Saadatmanesh H., Ehsani MR. RC beams strengthened with GFRP plates. I: experimental study. Journal of structural engineering 1991; 117(11): 3417-3433.

[2] Plevris N. and Triantafillou T.C. Strengthening of RC beams with epoxy-bonded fibre composite materials. Materials and Structures 1992; 25: 201-211.

[3] Capozucca R. Static and dynamic response of damaged RC beams strengthened with NSM CFRP rods. Composite Structures, 2009; 91: 237-248.

[4] Capozucca R. Analysis of the experimental flexural behaviour of a concrete beam grid reinforced with C-FRP bars. Composite Structures, 2007, 70(4): 517-526.

[5] Borri A., Castori G., Grazini A., Giannantoni A.. Composites SRP/SRG: characteristics, testing and applications. Building in Masonry, 2006; 117: 52-57 (in Italian).

[6] Huang X., Birman V., Nanni A., Tunis G. Properties and potential for application of steel reinforced polymer (SRP) and steel reinforced grout (SRG) composites. Composites Part B: Engineering, 2005; 36 (1): 73-82.

[7] Lopresto V., Leone C., De Iorio I. Mechanical characterization of basalt fibre reinforced plastic. Composites part B: Engineering, June 2011; 42 (4): 717-723.

[8] Militký J., Kovačič V., Bajzik V. Mechanical Properties of Basalt Filaments. Fibres & Textiles in Eastern Europe, 2007; 15 (5-6): 49-53.

[9] EC2 – UNI EN 1992-1-1:2005 Eurocode 2 - Design of concrete structures - Part 1-1: General rules and rules for buildings.

[10] Ugural A. C. Stresses in plates and shells. McGraw-Hill, London, 1981.